



Received: 18/10/2023
Original Research Article

Revised: 21/02/2024

Accepted: 18/03/2024

Published online: 29/03/2024



Open Access under the CC BY -NC-ND 4.0 license

UDC 537.322

SIMULATION OF MULTIPOINT CONTACT UNDER THERMOELECTRIC TESTING

Kostina M.A.¹, Soldatov A.I.¹, Soldatov A.A.¹, Abouellail A.A.²

¹National Research Tomsk Polytechnical University, Tomsk, Russia

²Sphinx University, New Asyut, Egypt

*Corresponding author: mariyakostina91@mail.ru

Abstract. The article presents the results of modeling a multipoint contact in the thermoelectric method of testing. Sources of thermoelectromotive force (thermoEMF) have shown different influences, according to their type, on the load characteristics of the equivalent source obtained by parallel connection of several thermocouples as shown in the explanatory figures. The presented model is implemented in the NI LabVIEW package, which is freely available. The model was verified on three types of thermocouples (copper-constantan, copper-nichrome, and chromel-alumel), which have been connected in parallel in different quantities. The calculated load characteristics of the equivalent sources differ from the experimental ones by no more than 6%. The results of modeling the load characteristics of the equivalent thermoEMF sources obtained by parallel connection of different quantities of two types of thermocouples are presented. It is shown that in order to obtain reliable data, it is necessary to provide an equivalent source load of at least 1 kOhm.

Keywords: thermos EMF, equivalent source, parallel connection, multipoint contact, load characteristics, superposition method.

1. Introduction

Thermoelectric testing is used in many areas of industrial production. One of the undoubted advantages of the thermoelectric method is the possibility of rapid testing. Another advantage is the simplicity of the technical implementation of this method, the compactness and autonomy of thermoelectric testing devices, ease of sample preparation, and intuitive testing procedure, which does not require special training of personnel. The main application area of the thermoelectric method is testing of metal products: sorting by steel grade, quality control of heat treatment, decarbonized layer, plastic deformation [1-20]. In scientific research, the thermoelectric method is used to measure the Seebeck coefficient [21].

A whole lineup of various thermoelectric devices is being produced for thermoelectric testing purposes. The Taiwanese company ACTTR produces Seebeck coefficient analyzer SETARAM SeebeckPro, the French company DIRECTINDUSTRY produces Seebeck coefficient and electrical resistance analyzer SR-3 Linseis, the German company NETZSCH produces NETZSCH SBA 458 Nemesis for thermoelectric testing, the Japanese company ADVENCE-RICO produces ULVAC ZEM-3 for measurement of the Seebeck coefficient and electrical conductivity, the English company QM-PLUS produces MMR Seebeck System for measuring the Seebeck coefficient of metals, the Russian company VELMAS produces a thermoelectric analyzer of metals and alloys TAMIS, and Tomsk Polytechnic University manufactures «THERMO FITNESS TESTING» for differential thermoelectric testing.

Despite the wide range of manufactured devices, all of them have disadvantages associated with low repeatability of test results [21 –22]. This can be attributed to the inhomogeneity of the surface of the tested sample in terms of chemical and phase composition. It should be noted that the influence of the heterogeneity of the chemical composition on thermoEMF is noted in the works of Karzhavin and Sungtaek [23, 24].

2. Formulation of the problem

To reduce the influence of such factors as inhomogeneity in chemical and phase composition, it was proposed to use electrodes with a linear or planar contact [25]. In this case, as the authors indicate, a multipoint contact is obtained. Each contact will be characterized by its own thermoEMF, as a result of alloyed iron, where carbides appear in the structure. Each point of contact will have different thermoelectric characteristics in relation to iron. The value of the carbide phase can vary from 5 to 30 % of the surface area of the sample, depending on the degree of alloying (Fig. 1) [26]. The equivalent thermoEMF will be determined by the parallel connection of these sources. Their number will depend on the size of the electrodes and the surface roughness (Fig. 2).

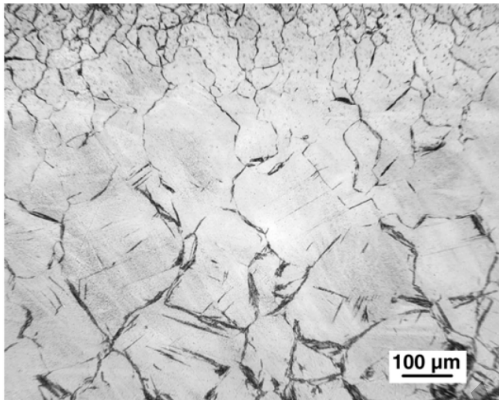


Fig.1. Carbides in alloy steel.

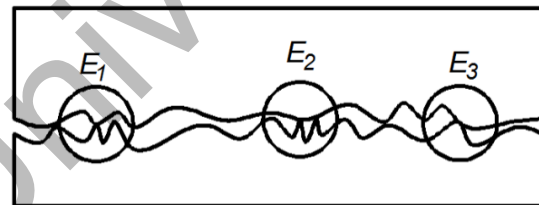


Fig.2. Projection of multi-point contact between the surfaces of the electrodes and the alloy steel

In this case, the equivalent thermoEMF is measured, which is composed of a parallel connection of thermoEMF sources with different thermoelectric characteristics: EMF value, internal resistance, power, and also different contact resistance. One approach to studying this mechanism is to use various types of thermocouples connected in parallel to simulate the circuit of multipoint contact (Fig. 3) [27-28].

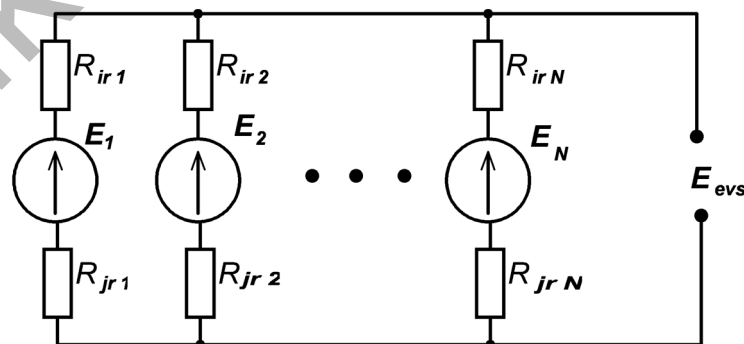


Fig.3. Equivalent electrical circuit for thermoelectric testing with a multipoint contact, $R_{ir1} \dots R_{irN}$ – internal resistances, $E_1 \dots E_N$ – EMF sources, $R_{jr1} \dots R_{jrN}$ – contact resistances, E_{evs} – equivalent EMF source

2. Model Development

The model development began with the circuit as a foundation, containing several thermoEMF sources connected in parallel to a common load (Fig. 4). Such a scheme reflects a multi-point contact, in which a thermoEMF source appears at each point of contact. In this case, taking into account the inhomogeneity in the chemical and phase composition of the surface of the tested sample, the characteristics of thermoEMF sources can be either the same or different.

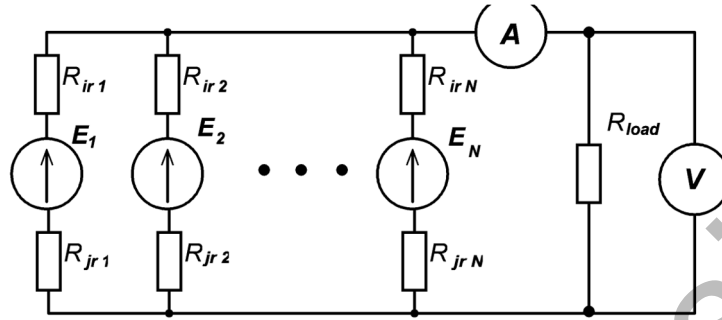


Fig.4. Equivalent circuit multipoint contact of the test sample with the electrode, $R_{ir1} \dots R_{irN}$ – internal resistances, $E_1 \dots E_N$ – EMF sources, $R_{jr1} \dots R_{jrN}$ – contact resistances, A – ammeter, V – voltmeter

The model algorithm implements the calculation of currents from each thermoEMF source based on the superposition method. The current flowing through the load from the first EMF source is determined by the formula:

$$I_1 = \frac{E_1}{(R_{ir1} + R_{jr1}) + \frac{R_{load} \prod_{i=2}^n (R_{iri} + R_{jri})}{R_{load} + \sum_{i=2}^n (R_{iri} + R_{jri})}}, \tag{1}$$

where I_1 is the current of the first thermoEMF source, E_1 is the EMF of the first source, R_{iri} is the internal resistance of the EMF source under the number i , R_{jri} is the contact resistance of the EMF source under the number i , and R_{load} is the load resistance.

The current flowing through the load from the second EMF source is determined by the formula:

$$I_2 = \frac{E_2}{(R_{ir2} + R_{jr2}) + \frac{R_{load} \cdot (R_{ir2} + R_{jr2}) \prod_{i=3}^n (R_{iri} + R_{jri})}{R_{load} + (R_{ir2} + R_{jr2}) + \sum_{i=3}^n (R_{iri} + R_{jri})}}, \tag{2}$$

where I_2 is the current of the second thermoEMF source and E_2 is the EMF of the second source.

In general terms, it can be written that the current flowing through the load from the k-th EMF source will be determined by the formula:

$$I_k = \frac{E_k}{(R_{irk} + R_{jrk}) + \frac{R_{load} \cdot \prod_{i=1}^{k-1} (R_{iri} + R_{jri}) \cdot \prod_{i=k+1}^n (R_{iri} + R_{jri})}{R_{load} + \sum_{i=1}^{k-1} (R_{iri} + R_{jri}) + \sum_{i=k+1}^n (R_{iri} + R_{jri})}}, \tag{3}$$

where I_k is the current of k-th thermoEMF source and E_k is the EMF of the k-th source.

The total current in the load (I_{load}) is the sum of the currents from all thermoEMF sources, it is also the current of the equivalent source:

$$I_{evs} = I_{load} = \sum_{i=1}^n I_i. \tag{4}$$

Through the current and internal resistance of an equivalent source, its EMF can be determined:

$$E_{\text{evs}} = I_{\text{evs}} \cdot R_{\text{ir}} \quad (5)$$

where R_{ir} is the internal resistance of the equivalent thermoEMF source; I_{evs} is the current of the equivalent thermoEMF source.

The load voltage can be found by Ohm's law:

$$U_{\text{load}} = I_{\text{load}} \cdot R_{\text{load}} \quad (6)$$

Using this technique, it is possible to calculate the load voltage, current and EMF of an equivalent source when any number of thermoEMF sources are connected in parallel.

3. Software Interface

The software was developed by NI LabVIEW software package. It calculates the load characteristics of the equivalent thermoEMF source when an unlimited number of parallel thermoelectric sources, that can have both the same and different characteristics. The obtained characteristics of the equivalent thermoEMF source can be used for further analysis. The user interface includes five different functional tabs (Figures 5-6). The "Read" tab is designed to launch a file from the database (Fig. 5). The database contains experimental data of thermoEMF sources (currents and internal resistances for 11 different values of load resistance under three different temperature conditions: 100 °C, 200 °C, 300 °C). The "Temp Database" field specifies a database file for temporary storage of current data that are used in the process of calculating the load characteristic of an equivalent thermoEMF source. The "Adding New Type" tab is responsible for adding characteristic data of new thermoEMF sources to be simulated. The "Edit" tab is intended for editing the initial values in the database in case of an error. The "Delete" tab is intended for deleting the recently added 6 columns of experimental data of thermoEMF sources. The Simulate tab is responsible for calculating and presenting the results. It contains function buttons such as "Temperature" to set the temperature, and "Number of type X" to select the desired number of thermopower sources to be investigated.

After adjusting the input data in accordance with the test condition, the program displays the calculated output data, such as the dependence of the load voltage "VL", load current, internal resistance and equivalent thermopower on the load resistance "RL" (Fig. 6).

RL	Type 0-100-R	Type 0-100-I	Type 0-200	Type 0-200-I	Type 0-300-R	Type 0-300-I	Type 1-100-R	Type 1-100-I
0.0100	0.6965	0.0044	0.7117	0.0097	0.7048	0.0154	0.1005	0.0318
0.0500	3.0789	0.0010	3.1046	0.0022	3.0683	0.0095	0.4362	0.0072
0.1000	5.4532	0.0006	5.4377	0.0013	5.3900	0.0020	0.7701	0.0040
0.5000	11.7059	0.0003	11.7496	0.0006	11.7102	0.0009	1.6679	0.0016
1.0000	14.8458	0.0002	13.9899	0.0005	14.1828	0.0007	2.2184	0.0011
3.3000	18.3857	0.0001	18.3930	0.0003	18.3929	0.0005	2.7434	0.0006
6.8000	20.0378	0.0001	19.8942	0.0003	20.1806	0.0004	3.0308	0.0004
10.0000	21.5294	0.0001	21.5709	0.0002	21.5831	0.0003	3.0557	0.0003
57.0000	21.6277	0.0000	21.7798	0.0001	21.7014	0.0001	3.0267	0.0001
100.0000	21.7099	0.0000	21.3153	0.0001	21.1913	0.0001	3.0563	0.0000
1000.0000	21.5446	0.0000	21.9116	0.0000	22.0994	0.0000	3.0675	0.0000
10000.0000	0.0000	0.0000	0.0000	0.0000	0.0000	0.0000	0.0000	0.0000

Fig.5. The "Read" tab in the program interface

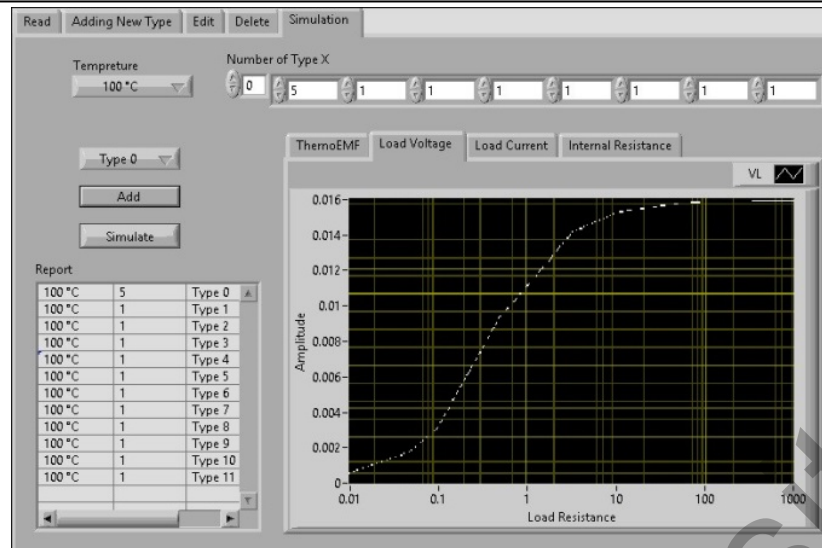


Fig.6. The “Adding New Type” tab in the program interface

The Add button is used to add new data to previous calculations. The "Simulate" button is used to start the simulation process. The simulation result is saved in a temporary file, which is indicated on the "Read" tab. The "Report" field displays the number of thermocouples that were used in the calculations.

4. Model verification

In order to verify the model, a set of experimental data is needed that reflects the electrical characteristics of typical thermoEMF sources and their combinations. Experimental studies were carried out on a specially made installation, which comprises a thermal chamber, in which investigated thermocouples are put, a voltmeter, a variable load, a microcontroller and a personal computer to control all the components of this installation [12, 29]. The thermocouples that are chosen to emulate experimental sources of thermoEMF are of types: copper-constantan, copper-nichrome and chromel-alumel. Fig. 7 shows the experimental characteristics of thermoEMF sources, each experimented individually: copper-nichrome, chromel-alumel, and copper-constantan.

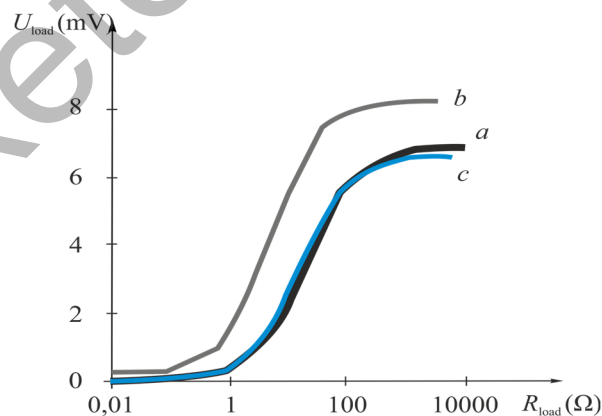


Fig.7. Experimental load characteristics of three thermocouples: (a) copper-constantan, (b) copper-nichrome, (c) chromel-alumel

The obtained characteristics of the three types of thermocouples were loaded into the developed simulation program and used to calculate the load characteristics of the equivalent thermoEMF source, which is composed of various combinations of the experimented thermocouple types. The influence of the copper-constantan thermocouple on the load characteristic of the equivalent thermoEMF source is presented in Fig.8.

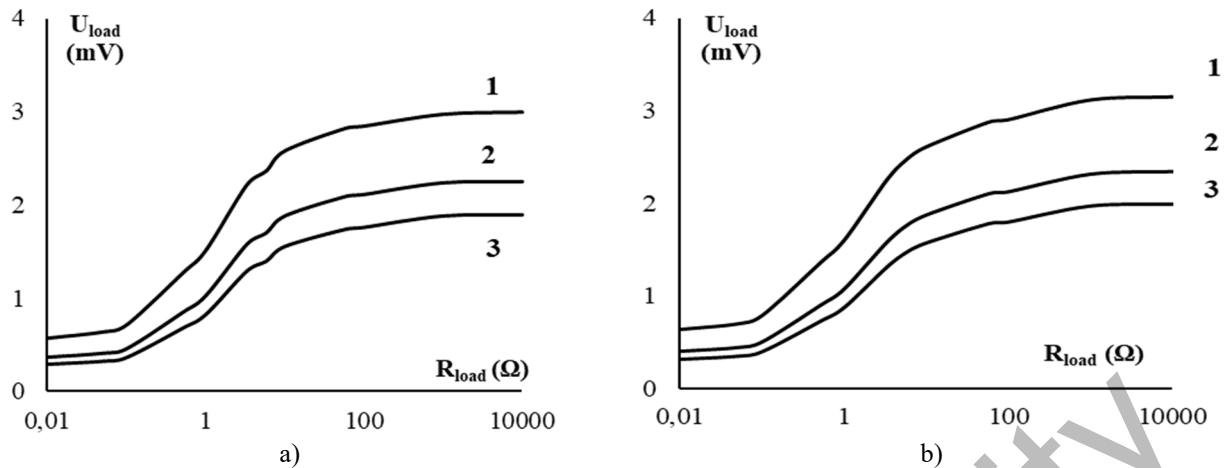


Fig.8. Load characteristics of equivalent thermopower sources for various combinations of thermocouples, (a) experimental results, (b) simulation results. Line No. 1, line No. 2, and line No. 3 indicate combinations of 4:4:4, 1:4:4, and 0:4:4, respectively. (the first digit in the thermocouple combination corresponds to the copper-constantan thermocouple, the second to copper-nichrome and the third to chromel-alumel)

Here Fig. 8.a shows the results of experimental studies, and Fig.8. b shows the results of program simulation. Line No. 1 in the figure indicates a combination of 4:4:4, line No. 2 indicates a combination of 1:4:4, and line No. 3 indicates a combination of 0:4:4.

The combinations indicate the number of thermocouples connected in parallel and their type. The first digit in the thermocouple combination corresponds to copper-constantan thermocouple, the second to copper-nichrome and the third to chromel-alumel, so the combination 4:4:4, for instance, means that four copper-constantan thermocouples, four copper-nichrome thermocouples and four chromel-alumel thermocouples were connected in parallel. The Fig.8 graphs shows a significant effect of copper-constantan thermocouple on the load characteristic of the equivalent thermoEMF source. The maximum value of thermoEMF is 3 mV for four thermocouples, 2.5 mV for one thermocouple and 1.9 mV for no thermocouple. The calculated values were 3.13 mV, 2.35 mV and 1.98 mV. The maximum deviation of the calculated data from the experimental ones did not exceed 6 %.

The influence of a chromel-alumel thermocouple on the load characteristic of the equivalent thermoEMF source is presented in Fig. 9, where Fig. 9.a shows the results of experimental studies, and fig. 9.b shows the results of simulation.

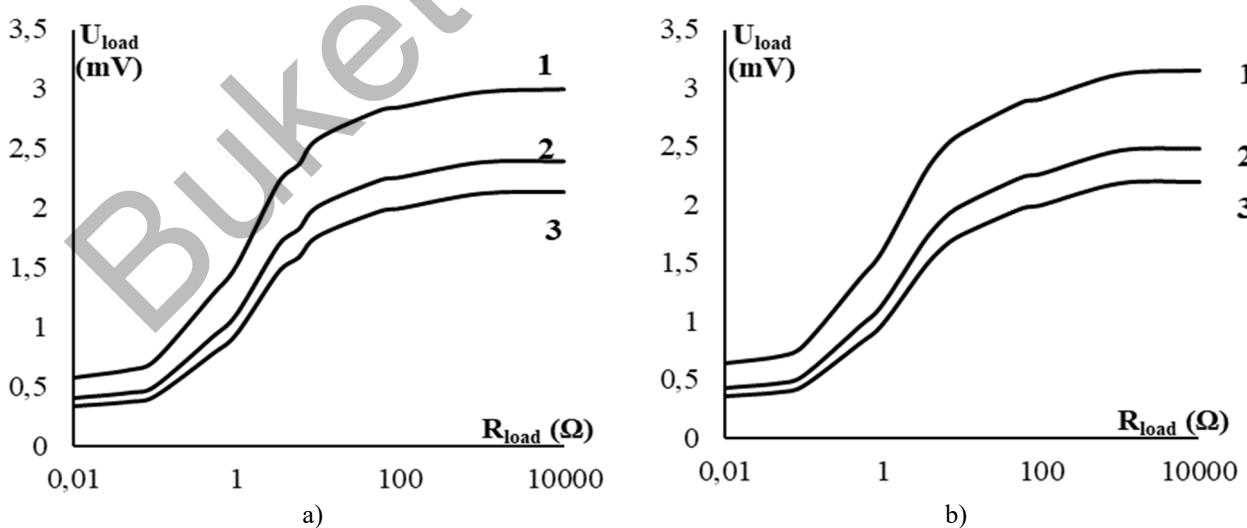


Fig.9. Load characteristic of an equivalent thermoEMF source for various combinations of thermocouples, (a) experimental results, (b) simulation results, line No. 1 - combination 4:4:4, line No. 2 - combination 4:4:1, line No. 3 - combination 4:4:0, (the first digit in the thermocouple combination corresponds to the copper-constantan thermocouple, the second to copper-nichrome and the third to chromel-alumel)

By studying the graphs of Fig. 9, we can conclude that chromel-alumel thermocouple has a noticeable effect on the load characteristic of the equivalent thermoEMF source. The maximum value of thermoEMF is 3 mV for four thermocouples, 2.39 mV for one thermocouple and 2.14 mV for no thermocouple. The calculated values were 3.13 mV, 2.49 mV and 2.19 mV. The maximum deviation of the calculated data from the experimental ones did not exceed 4.3 %.

The influence of copper-nichrome thermocouple on the load characteristic of the equivalent thermoEMF source is presented in Fig. 10, where Fig. 10.a shows the results of experimental studies, and figure 10.b shows the results of simulation.

By analyzing the graphs of Fig.10, we can conclude that chromel-alumel thermocouple has a noticeable effect on the load characteristic of the equivalent thermoEMF source. The maximum value of thermoEMF is 6.47 mV for four thermocouples, 4.89 mV for one thermocouple and 3 mV for no thermocouple. The calculated values were 6.46 mV, 5.1 mV and 3.15 mV. The maximum deviation of the calculated data from the experimental ones did not exceed 5 %. As can be seen from Figures 8-10, the model calculates the characteristics of equivalent thermoEMF sources with an error that does not exceed 6 %, and it can be used for further theoretical analysis.

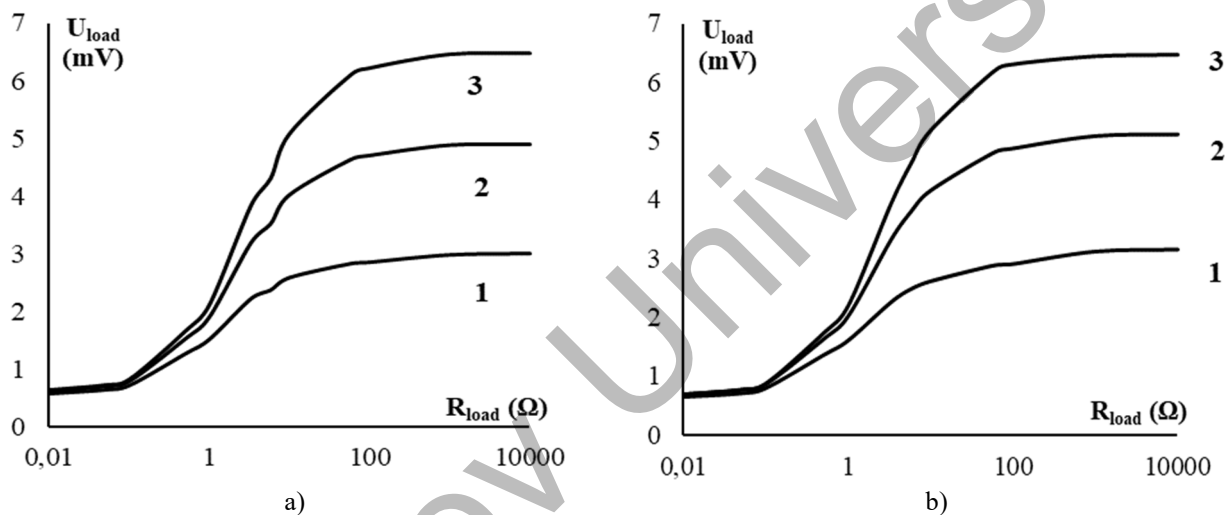


Fig.10. Load characteristic of an equivalent thermopower source for various combinations of thermocouples, (a) experimental results, (b) simulation results, line No. 1 - combination 4:4:4, line No. 2 - combination 4:1:4, line No. 3 - combination 4:0:4, (the first digit in the thermocouple combination corresponds to the copper-constantan thermocouple, the second to copper-nichrome and the third to chromel-alumel)

5. Theoretical Studies of Equivalent Thermoelectric Source Characteristics Caused by Multipoint-Contact Probing

Simulation of theoretical cases is important for studying possible properties that may arise due to the different characteristics of each thermoelectric source on the surface of the tested object in case of multipoint contact between the electrodes and the tested object. In other words, the value of thermoEMF of individual thermoelectric sources can vary over a wide range, which will lead to a change in the characteristics of the equivalent source.

Two types of thermoEMF sources (thermocouples) were used in the simulation. Their number in parallel connection is designated X:Y, where X is the number of thermocouples of the first type, and Y is the number of thermocouples of the second type. For example, the designation 1:1 corresponds to a parallel connection of one thermocouple of the first type and one thermocouple of the second type, and the designation 2:6 corresponds to a parallel connection of two thermocouples of the first type and six thermocouples of the second type. Fig. 11 shows the load characteristics of equivalent sources obtained from the simulation. In this case, two types of sources were used, differing in the thermoEMF value by 25 %.

Fig. 11 shows that at a load of more than 100 Ω, the deviation of the equivalent thermoEMF is no more than 12 % for any ratio of two types of thermoEMF sources connected in parallel. For a load of 1 kΩ, the deviation will be no more than 8 %.

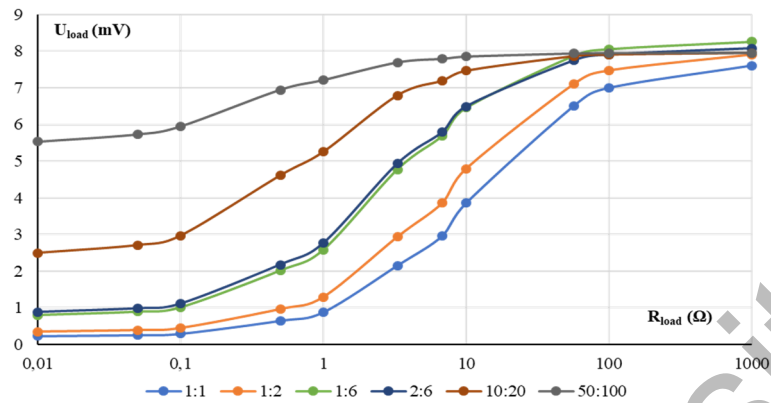


Fig.11. Load characteristics of an equivalent thermoEMF source obtained by parallel connection of two types of thermoEMF sources that differ by 25% (number of connected thermoEMF sources for the colored lines correspond to combination scales 1:1, 1:2, 1:6, 2:6, 10:20, 50:100)

Fig. 12 shows the characteristics of the equivalent source, obtained as a result of simulation, for two types of thermoEMF sources that differ in thermoEMF by 50 and 100 %.

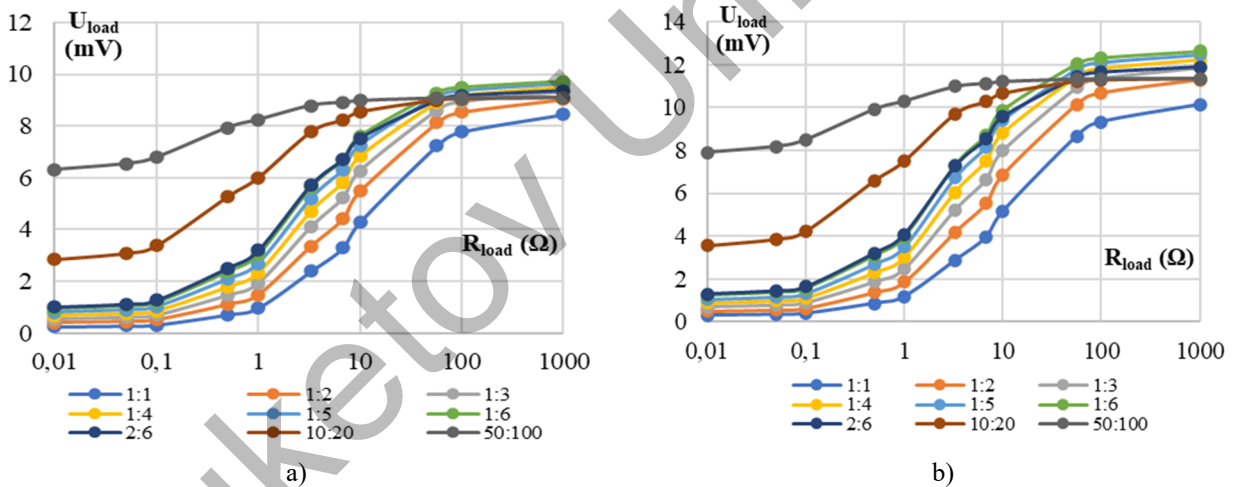


Fig.12. Dependence of the load voltage on the load resistance for an equivalent source obtained by parallel connection of two types of thermoEMF sources, differing by 50 % (a) and 100 % (b), (number of connected thermoEMF sources for the colored lines correspond to combination scales 1:1, 1:2, 1:6, 2:6, 10:20, 50:100)

As the number of parallel-connected thermoEMF sources increases, the absolute value of the equivalent thermoEMF increases. It can also be noted that the load resistance has a strong influence in the range from 0.01 to 50 Ohms on the value of the equivalent thermoEMF. In the range above 50 Ohms the influence decreases and at loads above 1 kOhm the differences are insignificant. Fig. 12 shows that at a load of more than 100 Ω, the deviation of the equivalent thermoEMF is no more than 6 % (Figure 12.a) and no more than 20 % (Figure 12.b) for any ratio of two types of thermoEMF sources connected in parallel. For a load of 1 kΩ, the deviation will be no more than 7 % (Fig. 12.a) and no more than 18 % (Fig. 12.b).

6. Experimental application

Experimental studies were carried out on the «THERMO FITNESS TESTING» device (Fig. 13.a). For the study, two grades of steel ShKh15 (Standard: GOST 801) and U8 (Standard: GOST 1435) were taken, from

which two samples were made for the study. One of the two samples served as a reference, and the other as a tested steel product. To obtain contact close to a point, the sensor was placed at an angle to both samples, so that there was only one point of contact (Fig. 13.b). To obtain a planar contact (in our case, a linear contact was obtained), the contact line of the sensor was placed parallel to one of the surfaces of each sample. The size of the contact line of the sensor with the samples was 10 mm, which, with the surface roughness of the sensor and the manufactured samples Rz 100, provided about 50 to 100 contact points.

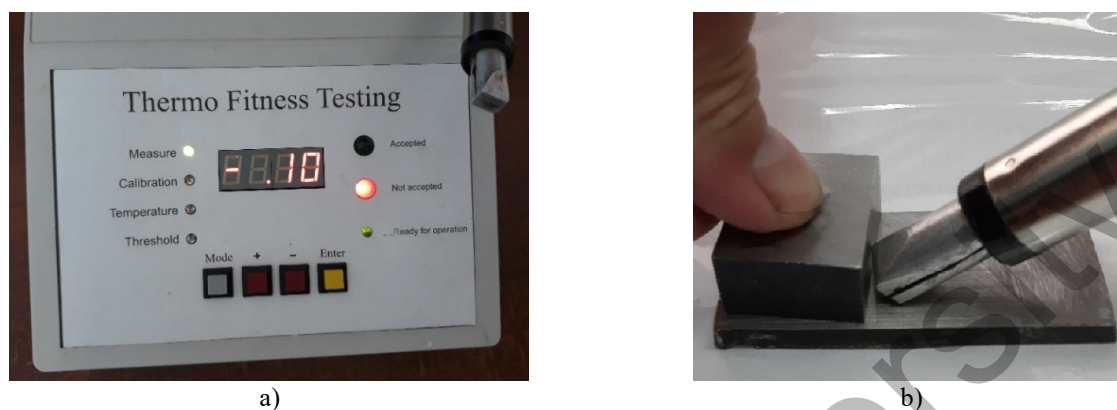


Fig.13. «THERMO FITNESS TESTING» thermoelectric testing device, a – electronics unit with sensor, b – location of the sensor and samples during testing

The main technical characteristics of the thermoelectric testing device for metals and alloys «THERMO FITNESS TESTING» are given in Table 1. It should be noted that thermoelectric testing devices are indicator-type devices.

Table 1. Technical characteristics of the device «THERMO FITNESS TESTING».

No.	Parameter name	Unit measurements	Value
1	Supply voltage	Volt	220
2	Sensor temperature setting range	Degree Celsius	50 ... 170
3	Accuracy of maintaining the set sensor temperature	Degree Celsius	± 5
4	Threshold voltage setting limits during sorting	μV	0,01...0,4
5	ThermoEMF measurement range	μV	0... $\pm 9,99$
6	Device readiness time	minutes	15
7	Turning on the “Accepted” signal		EMF is less than threshold voltage
8	Turning on the “Not accepted” signal		EMF is greater than threshold voltage

The results of experimental studies using the «THERMO FITNESS TESTING» showed that the differential thermoEMF fluctuations were $\pm 0.42 \mu\text{V}$ for ShKh15 when implementing a contact close to a point contact and $\pm 0.14 \mu\text{V}$ for a planar contact. For U8 steel, respectively, $\pm 0.31 \mu\text{V}$ for a point contact and $\pm 0.12 \mu\text{V}$ for a planar contact. Thus, the conducted studies confirmed the prospects of using electrodes with planar contact to reduce the influence of inhomogeneity of the chemical composition on the result of measuring thermoEMF.

7. Conclusion

The conducted studies have shown the importance of taking into account the thermoelectric characteristics of various chemical compounds that are on the surface of the test object. To obtain high repeatability of test results, it is necessary to increase the load resistance of an equivalent thermoEMF source. Under the circumstances of thermoEMF sources with load characteristics differing up to 50 %, the load resistance should be more than 1 k Ω . In this case, the deviation of the maximum thermoEMF value of

the equivalent source will be no more than 10 % for any number of thermoEMF sources connected in parallel. With large differences in the load characteristics of different thermoEMF sources (up to 100 %), the deviation of the maximum thermoEMF value for an equivalent source will be about 20 % for any number of thermoEMF sources connected in parallel. In addition, to ensure a fluctuation of less than 5%, it is necessary to have at least 10 points of contact of each electrode of the testing probe with the test sample, and the load resistance must be equal to or greater than 1 kOhm. However, if the value load resistance is 100 Ohms, then the number of contact points should be more than 30.

The conducted studies also showed the same nature of the dependence of the voltage on the load for three different types of thermoEMF sources: copper-constantan, copper-nichrome and chromel-alumel. A similar nature of the dependence is also observed for equivalent thermoEMF sources formed by various combinations of these thermocouples.

Conflict of interest statement

The authors declare that they have no conflict of interest in relation to this research, whether financial, personal, authorship or otherwise, that could affect the research and its results presented in this paper.

CRedit author statement

Kostina M.A.: Formal analysis; Soldatov A.I.: Conceptualization, Methodology, Project administration; Soldatov A.A.: Investigation, Validation; Abouellail A.A.: Software

The final manuscript was read and approved by all authors.

References

- 1 Paul E.M. *Introduction to Nondestructive Testing: A Training Guide, Second Edition*. John Wiley & Sons. 2005, 712 p. https://books.google.ru/books?id=LtIFcoeIP-UC&printsec=frontcover&redir_esc=y#v=onepage&q&f=false
- 2 Nagy P.B. Non-destructive methods for materials' state awareness monitoring. *Insight: Non-Destructive Testing and Condition Monitoring*, 2010, Vol. 52, Is.2, pp. 61-71. <https://doi.org/10.1784/insi.2010.52.2.61>
- 3 Soldatov A.A., Seleznev A.I., Fiks I.I., Soldatov A.I., Kröning Kh.M. Nondestructive proximate testing of plastic deformations by differential thermal EMF measurements. *Russian Journal of Nondestructive Testing*, 2012, Vol. 48, Is.3, pp. 184-186. <https://doi.org/10.1134/S1061830912030060>
- 4 Li J.F., Liu W.S., Zhao L.D., Zhou M. High-performance nanostructured thermoelectric materials. *Npg Asia Mater*, 2010, Vol. 2, Is.4, pp. 152-158. <https://doi.org/10.1038/asiamat.2010.138>
- 5 Kikuchi M. Dental alloy sorting by the thermoelectric method. *European Journal of Dentistry*, 2010, Vol. 4, No.1, pp.66-70. <https://www.ncbi.nlm.nih.gov/pmc/articles/PMC2798792/>
- 6 Cooper R.F. Sorting mixed metals by the thermoelectric effect. *Physics Education*, 1976, Vol. 11, Is.4, pp. 290-292. <https://doi.org/10.1088/0031-9120/11/4/004>
- 7 Stuart C. Thermoelectric Differences Used for Metal Sorting. *Journal of Testing and Evaluation*, 1987, Vol. 15, No. 4, pp. 224-230. <https://doi.org/10.1520/JTE11013J>
- 8 Dragunov V.K., Goncharov A.L. New approaches to the rational manufacturing of combined constructions by EBW. *IOP Conference Series: Materials Science and Engineering*, 2019, Vol. 681, pp. 012010. <https://doi.org/10.1088/1757-899X/681/1/012010>
- 9 Goncharov A., Sliva A., Kharitonov I., Chulkova A., Terentyev E. Research of thermoelectric effects and their influence on electron beam in the process of welding of dissimilar steels. *IOP Conference Series: Materials Science and Engineering*, 2020, Vol. 759, Is.1, pp. 012008. <https://doi.org/10.1088/1757-899X/759/1/012008>
- 10 Kharitonov I.A., Rodyakina R.V., Goncharov A.L. Investigation of magnetic properties of various structural classes steels in weak magnetic fields characteristic for generation of thermoelectric currents in electron beam welding. *Solid State Phenomena*, 2020, Vol. 299, pp. 1201-1207. <https://doi.org/10.4028/www.scientific.net/SSP.299.1201>
- 11 Soldatov A.I., Soldatov A.A., Kostina M.A., Kozhemyak O.A. Experimental studies of thermoelectric characteristics of plastically deformed steels ST3, 08KP and 12H18N10T. *Key Engineering Materials*, 2016, Vol. 685, pp. 310-314. <https://doi.org/10.4028/www.scientific.net/KEM.685.310>
- 12 Soldatov A.I., Soldatov A.A., Sorokin P.V., Abouellail A.A., Obach I.I., Bortalevich V.Y., Shinyakov Y.A., Sukhorukov M.P. An experimental setup for studying electric characteristics of thermocouples. *SIBCON 2017 - Proceedings*, 2017, pp. 79985342017. <https://doi.org/10.1109/SIBCON.2017.7998534>
- 13 Fulton J.P., Wincheski B., Namkung M. Automated weld characterization using the thermoelectric method. *Review of Progress in Quantitative Nondestructive Evaluation*, 1993, pp. 1611-1618. http://wayback.archive-it.org/1792/20100511094916/http://ntrs.nasa.gov/archive/nasa/casi.ntrs.nasa.gov/20040129656_2004126555.pdf

- 14 Carreon H., Medina A. Nondestructive characterization of the level of plastic deformation by thermoelectric power measurements in cold-rolled Ti–6Al–4V samples. *Nondestructive Testing and Evaluation*, 2007, Vol. 22, Is. 4, pp. 299-311. <https://doi.org/10.1080/10589750701546960>
- 15 Carreon M. Thermoelectric detection of fretting damage in aerospace materials. *Russian Journal of Nondestructive Testing*, 2013, Vol. 50, Is.11, pp. 86940Z. <https://doi.org/10.1117/12.2009448>
- 16 Lakshminarayan B., Carreon H., Nagy P. Monitoring of the Level of Residual Stress in Surface Treated Specimens by a Noncontacting Thermoelectric Technique. *AIP Conference Proceeding*, 2003, Vol. 657, pp. 1523-1530. <https://doi.org/10.1063/1.1570311>
- 17 Carreon H. Evaluation of Thermoelectric Methods for the Detection of Fretting Damage in 7075-T6 and Ti-6Al-4V Alloys. *Characterization of Minerals, Metals, and Materials*, 2015, pp. 435–442. https://doi.org/10.1007/978-3-319-48191-3_53
- 18 Carreon M., Barriuso S., Barrera G., González-carrasco J. L., Caballero F. Assessment of blasting induced effects on medical 316 LVM stainless steel by contacting and non-contacting thermoelectric power techniques. *Surface and Coatings Technology*, 2012, Vol. 206, pp. 2942-2947. <https://doi.org/10.1016/j.surfcoat.2011.12.026>
- 19 Hu J., Nagy P.B. On the Thermoelectric Effect of Interface Imperfections. *Review of Progress in Quantitative Nondestructive Evaluation*, 1999, Vol. 188, pp. 1487-1494. https://doi.org/10.1007/978-1-4615-4791-4_191
- 20 Ciylan B., Yılmaz S. Design of a thermoelectric module test system using a novel test method. *International Journal of Thermal Sciences*, 2007, Vol. 46, Is.7, pp. 717-725. <https://doi.org/10.1016/j.ijthermalsci.2006.10.008>
- 21 Zhou Y. and et al. Fast Seebeck coefficient measurement based on dynamic method. *Rev. Sci. Instrum.* 2014, Vol. 85, Is. 5, pp. 054904. <https://doi.org/10.1063/1.4876595>
- 22 Hu J., Nagy P.B. On the role of interface imperfections in thermoelectric nondestructive materials characterization. *Applied Physics Letters*, 1998, Vol. 73, pp. 467-469. <http://dx.doi.org/10.1063/1.121902>
- 23 Karzhavin V.A. *The influence of thermoelectric inhomogeneity on the accuracy of temperature measurement by thermocouples [Vlijanie termojelektricheskoy neodnorodnosti na tochnost' izmereniya temperatury termoparami]*. Candidate Diss. of the Techn. Science degree, Obninsk, 2010, 148 p. [in Russian]
- 24 Metals determinant thermoelectric OMET. Passport. Technical description Manual. [in Russian] Available at: <https://analyzer24.ru/brosh/port-analiz/OMET/OMET.pdf>
- 25 Sungtaek Ju Y. Study of interface effects in thermoelectric microrefrigerators. *Journal of Applied Physics*, 2000, Vol. 88, Is.7, pp. 4135 – 4139. <https://doi:10.1063/1.1289776>
- 26 Abouellail A.A., Chang, J., Soldatov, A.I., Soldatov, A.A., Kostina, M.A., Bortalevich, S.I., Soldatov, D.A. Influence of Destabilizing Factors on Results of Thermoelectric Testing. *Russian Journal of Nondestructive Testing*, 2022, Vol. 58, Is. 7, pp. 607–616. <https://doi.org/10.1134/S1061830922070026>
- 27 Hetzner D.W., Van Geertruyden W. Crystallography and metallography of carbides in high alloy steels. *Materials Characterization*, 2008, Vol. 59, pp. 825 – 841. <https://doi:10.1016/j.matchar.2007.07.005>
- 28 Corcoran J., Raja S., Nagy, P. Improved thermoelectric power measurements using a four-point technique. *NDT & E International*, 2017, Vol. 94, pp. 92-100. <https://doi:10.1016/j.ndteint.2017.12.002>
- 29 Abouellail A.A., Obach I.I., Soldatov A.A., Soldatov A.I. Surface inspection problems in thermoelectric testing. *MATEC Web of Conferences*, 2017, Vol. 102, pp. 01001. <https://doi:10.1051/mateconf/201710201001>

AUTHORS' INFORMATION

Kostina, M.A. – Candidate of techn. sciences, Associate Professor, National Research Tomsk Polytechnical University, Tomsk, Russia; ORCID ID: 0000-0003-2626-6002; mariyakostina91@mail.ru

Soldatov, A.A. – Candidate of techn. sciences, Associate Professor, National Research Tomsk Polytechnical University, Tomsk, Russia; ORCID ID: 0000-0003-0696-716X; soldatov.88@bk.ru

Soldatov, A.I. – Doctor of techn. sciences, Professor, National Research Tomsk Polytechnical University, Tomsk, Russia, Tomsk, Russia; ORCID ID: 0000-0003-1892-1644; asoldatof@mail.ru

Abouellail, A.A. - Candidate of techn. sciences, Lecturer, Sphinx University, New Asyut, Egypt; ORCID ID: 0000-0002-9357-6214; ahmed.abouellail@sphinx.edu.eg